

$$\begin{aligned}
 H = & \sum_{i=1,2}^{n+2} \omega_i |i\rangle\langle i| + E_P(t) [\mu_{1,2} |1\rangle\langle 2| + \text{H.c.}] \\
 & + E_D(t) \sum_{k=3}^{n+2} [\mu_{2,k} |2\rangle\langle k| + \text{H.c.}] + H_{\text{int}}. \quad (1)
 \end{aligned}$$

The total pump (P) and dump (D) electric fields are

$$\begin{aligned}
 E_P(t) &= \text{Re}(\mathcal{E}_{1,2}(t) \exp(-i\omega_{1,2}t)), \quad (2) \\
 E_D(t) &= \text{Re}\left(\sum_{k=3}^{n+2} \mathcal{E}_{2,k}(t) \exp(-i\omega_{2,k}t)\right),
 \end{aligned}$$

where the slow field amplitudes $\mathcal{E}_{i,j}(t)$ in the dump field have the *same* smooth (Gaussian) time profile. This profile determines the envelope of the dump field $E_D(t)$, which is fast modulated by interferences of the many present frequency components. The frequencies $\omega_{i,j}$ in the fields $E_P(t)$

and $E_D(t)$ are chosen such as to fit the distances between the levels of the SAP scheme ($\omega_{i,j} \approx \omega_i - \omega_j$), and resonantly couple states $|1\rangle$ and $|2\rangle$, and state $|2\rangle$ with states $|k\rangle$ ($k = 3, \dots, n+2$) via the dipole matrix elements $\mu_{1,2}$ and $\mu_{2,k}$, respectively. Finally, H_{int} in Eq. (1) includes the terms responsible for scattering and relaxation.

The system evolution is described by the wave function $|\Psi\rangle = \sum_{i=1}^{n+2} c_i(t) e^{-i\omega_i t} |i\rangle$. The column vector of $c_i(t)$ ($i = 1, \dots, n+2$) coefficients,

$$\mathbf{c}(t) = (c_1, c_2, c_3, \dots, c_{n+2})^T, \quad (3)$$

where T designates the matrix transpose, is a solution of the matrix Schrödinger equation

$$\dot{\mathbf{c}}(t) = -i\mathbf{H}(t)\mathbf{c}(t) \quad (4)$$

with the Hamiltonian ($\delta_{i,j} = \omega_j - \omega_i$)

$$\mathbf{H}(t) = \begin{bmatrix} 0 & E_P(t)\mu_{1,2}e^{-i\delta_{1,2}t} & 0 & \dots & 0 \\ E_P(t)\mu_{2,1}e^{i\delta_{1,2}t} & 0 & E_D(t)\mu_{2,3}e^{-i\delta_{2,3}t} & \dots & E_D(t)\mu_{2,n+2}e^{i\delta_{2,n+2}t} \\ 0 & E_D(t)\mu_{3,2}e^{i\delta_{2,3}t} & 0 & \dots & 0 \\ \dots & \dots & \dots & \dots & \dots \\ 0 & E_D(t)\mu_{n+2,2}e^{i\delta_{2,n+2}t} & 0 & \dots & 0 \end{bmatrix}. \quad (5)$$

We make the rotating wave approximation in $\mathbf{H}(t)$, but retain those components of the dump electric field, which are close in frequency. This leads to the effective SAP Hamiltonian

$$\mathbf{H}_{\text{SAP}}(t) = \begin{bmatrix} 0 & \Omega_{1,2} & 0 & \dots & 0 \\ \Omega_{2,1} & 0 & \Sigma_{2,3} & \dots & \Sigma_{2,n+2} \\ 0 & \Sigma_{3,2} & 0 & \dots & 0 \\ \dots & \dots & \dots & \dots & \dots \\ 0 & \Sigma_{n+2,2} & 0 & \dots & 0 \end{bmatrix}, \quad (6)$$

where $\Omega_{i,j}(t) \equiv |\Omega_{i,j}(t)| e^{i\phi_{i,j}} \equiv \mu_{i,j} \mathcal{E}_{i,j}(t)$ are the Rabi frequencies and $\Sigma_{2,k}(t)$ are their (dump) modifications,

$$\begin{aligned}
 \Sigma_{2,k}(t) &= \mu_{2,k} \sum_{l=3}^{n+2} \exp[-i(\delta_{2,k} + \omega_{2,l})t] \mathcal{E}_{2,l}(t) \\
 &= \Omega_{2,k}(t) + (\text{off-resonant terms}). \quad (7)
 \end{aligned}$$

These elements $\Sigma_{2,k}$ incorporate the effects of both the on-resonance, $\mathcal{E}_{2,k}$ ($\delta_{2,k} + \omega_{2,k} \approx 0$), and the “weakly” off-resonance, $\mathcal{E}_{2,l \neq k}$ ($\delta_{2,k} + \omega_{2,l} \approx \omega_k - \omega_l$), field components on a given $|k\rangle \leftarrow |2\rangle$ transition.

Eigenvalues and eigenvectors

Of the $n+2$ eigenvalues of $\mathbf{H}_{\text{SAP}}(t)$, n are zero and two are nonzero,

$$\lambda_{1,2,\dots,n} = 0,$$

$$\lambda_{n+1,n+2}(t) = \pm \left(|\Omega_{1,2}(t)|^2 + \sum_{k=3}^{n+2} |\Sigma_{2,k}(t)|^2 \right)^{1/2}. \quad (8)$$

The zero eigenvalues correspond to the n null (often called “dark”) states,

$$|D_{k-2}\rangle = \Sigma_{2,k} |1\rangle - \Omega_{2,1} |k\rangle, \quad (k = 3, \dots, n+2), \quad (9)$$

mixing the initial $|1\rangle$ state and the final $|k\rangle$ states. We use basis vectors redefined as $e^{-i\omega_j t} |j\rangle \rightarrow |j\rangle$

If the field components $\mathcal{E}_{i,j}(t)$ change slowly enough with time, such that,

$$\left(\mathbf{U}^{-1}(t) \frac{d}{dt} \mathbf{U}(t) \right)_{k,l} \ll |\lambda_k(t) - \lambda_l(t)|, \quad (10)$$

where $\mathbf{U}(t)$ is the matrix of eigenvectors, we expect the *adiabatic* solution, based on diagonalizing \mathbf{H}_{SAP} , to be accurate. In addition, when the field components are relatively weak and change slowly in time, so the pulse is long with respect to the vibrational period $\tau_{\text{vib}} \approx 1/|\omega_i - \omega_{i\pm 1}| \ll 1/|\Omega_{ij}| \ll \tau_{\text{pulse}}$, the contributions of the off-resonance oscillatory terms of Eq. (7) should average out, causing $\Sigma_{2,k}(t)$ to coincide with the resonant term, $\Omega_{2,k}(t)$.

Let us examine first a SAP scheme with $n=2$ and approximate $\Sigma_{2,k}$ by $\Omega_{2,k}$. As found in the past [32,33], in this four-level model the final adiabatic branching ratio between state $|3\rangle$ and state $|4\rangle$ is given by $|\Omega_{3,2}/\Omega_{4,2}|^2$ (as in first-order perturbation theory). Here, we exactly reexamine why this system gives such a robust output, even though the adiabatic condition in Eq. (10) with two null eigenvalues cannot be valid (right-hand side is zero).

We execute a linear transformation within the null subspace, such that one null eigenvector has the form [34],

$$|D'_1\rangle = \sum_{k=3}^4 \Omega_{k,2} |D_{k-2}\rangle = |1\rangle \sum_{k=3}^4 |\Omega_{k,2}|^2 - \Omega_{2,1} \sum_{k=3}^4 \Omega_{k,2} |k\rangle, \quad (11)$$

and the other null eigenvector is given as,

$$|D'_2\rangle = \Omega_{2,4} |D_1\rangle - \Omega_{2,3} |D_2\rangle = \Omega_{2,1} (\Omega_{2,3} |4\rangle - \Omega_{2,4} |3\rangle), \quad (12)$$

so the two are always orthogonal

$$\langle D'_1 | D'_2 \rangle = |\Omega_{2,1}|^2 (\Omega_{3,2}^* \Omega_{2,4} - \Omega_{4,2}^* \Omega_{2,3}) \equiv 0. \quad (13)$$

The two non-null eigenstates

$$\begin{aligned} |D'_3\rangle &= \Omega_{1,2} |1\rangle + \lambda |2\rangle + \Omega_{3,2} |3\rangle + \Omega_{4,2} |4\rangle, \\ |D'_4\rangle &= \Omega_{1,2} |1\rangle - \lambda |2\rangle + \Omega_{3,2} |3\rangle + \Omega_{4,2} |4\rangle, \\ \lambda &= \sqrt{|\Omega_{1,2}|^2 + |\Omega_{2,3}|^2 + |\Omega_{2,4}|^2} \end{aligned} \quad (14)$$

are also orthogonal to each other $\langle D'_3 | D'_4 \rangle \equiv 0$ and to the null states $\langle D'_i | D'_j \rangle \equiv 0$ ($i=1,2$ and $j=3,4$).

We can now transform the Schrödinger equation (4) to the space of eigenstates [32–34], with the four-state basis $|D'_i\rangle$ ($i=1-4$). The transformed equation is

$$\dot{\mathbf{v}}(t) = -i\mathbf{W}(t)\mathbf{v}(t), \quad (15)$$

where $\mathbf{v}(t) = \mathbf{U}^{-1}(t)\mathbf{c}(t)$ is the new state vector. The matrix $\mathbf{U}(t)$ of eigenvectors diagonalizes the Hamiltonian (6) and generates the evolution matrix

$$\mathbf{W}(t) \equiv \mathbf{U}^{-1}(t)\mathbf{H}(t)\mathbf{U}(t) + i\dot{\mathbf{U}}^{-1}(t)\mathbf{U}(t). \quad (16)$$

If we calculate this evolution matrix $\mathbf{W}(t)$, we realize that it *does not* couple at all the $|D'_1\rangle$ and $|D'_2\rangle$ states, i.e., from the elements $W_{ij}(t)$ ($i,j=1,2$) only $W_{11}(t) \neq 0$. This is the crucial fact, which explains the robustness of the above result $p_3/p_4 = |\Omega_{3,2}/\Omega_{4,2}|^2$, even when Eq. (10) is broken due to the two-dimensional null subspace.

Let us see why. In the counterintuitive pulse-ordering scheme, where $\Omega_{2,k}(t)$ precedes $\Omega_{2,1}(t)$, *only* the null state $|D'_1\rangle$ correlates initially with the state $|1\rangle$; in contrast, the null state $|D'_2\rangle$ is orthogonal to $|1\rangle$ at all times and the non-null states $|D'_3\rangle$, $|D'_4\rangle$ are orthogonal to $|1\rangle$ at the *beginning* ($t=0$). Thus, in the adiabatic evolution starting from state $|1\rangle$, we can directly decouple the two non-null eigenstates in Eq. (15), by setting $W_{ij}(t) = 0$ ($i,j=3,4$), and still obtain an

essentially exact evolution [32–34]. Since from the rest elements only $W_{11}(t) \neq 0$, all the population *must* remain in the null state $|D'_1\rangle$. But in this state $|D'_1\rangle$, the transition amplitudes c_3 and c_4 , of the finally populated states $|3\rangle$ and $|4\rangle$, are proportional to the Rabi frequencies $\Omega_{3,2}$ and $\Omega_{4,2}$, respectively, so the final populations of these two states $|k\rangle$ ($k=3,4$), given as $p_k = |c_k|^2$, are proportional to $|\Omega_{k,2}|^2$.

We can now return to the general $[(n+2)$ -level] SAP system and transform, in analogy to the above, the null states such that in the counterintuitive pulse-ordering scheme, only one of these transformed states correlates initially with state $|1\rangle$,

$$|D'_1\rangle = |1\rangle \sum_{k=3}^{n+2} |\Omega_{k,2}|^2 - \Omega_{2,1} \sum_{k=3}^{n+2} \Omega_{k,2} |k\rangle, \quad (17)$$

with the other null states kept orthogonal to state $|1\rangle$. Since only this $|D'_1\rangle$ gets adiabatically populated, it follows immediately from Eq. (17) that $c_k \propto \Omega_{k,2}$ and $p_k = |c_k|^2 \propto |\Omega_{k,2}|^2$. This is exactly the result of the first-order perturbation theory [2,6,17], which holds here even in the strong field regime.

III. VIBRATIONAL SAP IN THE Na₂ MOLECULE

As an example of SAP, we now examine Raman transitions in the Na₂ molecule [36]. In particular, we look at a process in which, using a Raman transition starting from the $v=0$ vibrational state of the $X^1\Sigma_g^+$ ground electronic state, we populate a superposition of high lying v vibrational states of the *same* electronic state, using the $v'=0$ vibrational level of the *excited* electronic state $A^1\Sigma_u^+$ as an intermediate state. As our target we choose to populate a “coherent-state” wave packet given as

$$|\alpha\rangle = \exp\left(-\frac{1}{2}|\alpha|^2\right) \sum_{v=0}^{\infty} \frac{\alpha^v}{(v!)^{1/2}} |v\rangle, \quad (18)$$

although the excitation of other interesting superposition states, such as the displaced and squeezed Fock states [37], should be also feasible.

In principle, we can also generate vibrational coherent states belonging to other electronic states. Having, however, chosen to start and end in the same electronic state, means that we have to limit somewhat the range of α values that can be considered, because we need to exclude the $|v=0\rangle$ state from our superposition. This is due to the fact that the $|v=0\rangle$ state also serves as our initial state and its use as part of the target manifold would invalidate the form of the Hamiltonian used in Eq. (6). Even for α values as low as -3 the exclusion of the $|v=0\rangle$ state does not detract much from achieving our objective, because the weight of the $|v=0\rangle$ state in $|\alpha=-3\rangle$ state is very small.

A. Shaping the pulse

Following the above arguments, the pulse shape needed to attain the target wave packet of Eq. (18) is of the form,

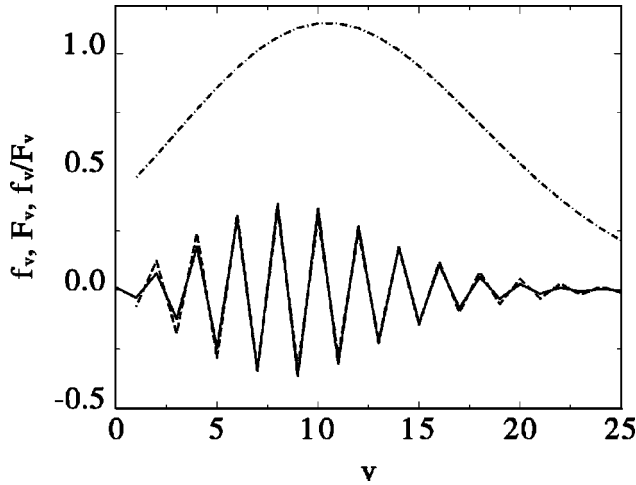


FIG. 2. Creation of Na_2 coherent states in the $A^1\Sigma_u^+ \leftarrow X^1\Sigma_g^+$ electronic transition. Solid line, the amplitudes $f_v = \alpha^v / (v!)^{1/2}$. Dashed line, the FC coefficients $F_v = \langle v'=0 | v \neq 0 \rangle$. Dot-dashed line, The f_v/F_v ratio, proportional to the $\mathcal{E}_{2,v+2}(t)$ field components.

$$\mathcal{E}_{2,k=v+2}(t) = \frac{f(t)\alpha^v}{(v!)^{1/2}\mu_{2,v+2}}, \quad (19)$$

where $f(t)$ is an arbitrary smooth function of the time. Following the Franck-Condon approximation [38] we approximate the transition-dipole matrix elements as,

$$\mu_{2,v+2} \equiv \langle A^1\Sigma_u^+, v'=0 | \hat{\epsilon} \cdot \mu | X^1\Sigma_g^+, v \rangle \approx \bar{\mu} \langle 0 | v \rangle,$$

where $\hat{\epsilon}$ is the polarization direction and $\bar{\mu}$ a constant number representing an “average” electronic transition dipole moment. The $\langle 0 | v \rangle$ overlap integrals are called the “Franck-Condon” (FC) factors [38]. For the above transition $\bar{\mu} \approx 7$ D [39].

The pulse of Eq. (19) is expected to attain the desired objective because $c_k \propto \Omega_{2,k} = \mu_{2,k} \mathcal{E}_{2,k}(t) \propto \alpha^v / (v!)^{1/2}$, $v=k-2$, as required by Eq. (18). Experimentally, it is possible to shape pulses using 128–256 discrete (equidistant) frequencies [22,24]. Therefore, a nearly coherent state composed of as many as 10–20 (slightly anharmonic) vibrational levels can be generated. For more complex wave packets, the number of levels (hence, frequencies) necessary to achieve good overlap with the target would be higher.

In Fig. 2, we compare the amplitudes of the chosen coherent state (18) in terms of Fock states, $f_v = \alpha^v / (v!)^{1/2}$, with $\alpha = -3$ (solid line), with the FC coefficients $F_v = \langle v'=0 | v \neq 0 \rangle$ between the vibrational wave functions of the $A^1\Sigma_u^+$ and $X^1\Sigma_g^+$ states (dashed line). We have chosen the vibrational vacuum $|v'=0\rangle$ of $A^1\Sigma_u^+$ as the intermediate state $|2\rangle$, so that *none* of the FC factors is too small (necessitating the use of very large electric-field components). Because the $A^1\Sigma_u^+ |v'=0\rangle$ vibrational state is a nearly perfect Gaussian function, from the point of view of the ground $X^1\Sigma_g^+$ state dynamics it appears as a coherent state, slightly shifted from the equilibrium position. Hence, the values of the FC factors

and the expansion coefficients of an $\alpha = -3$ coherent state in the Fock states are very similar. As a result, their ratio (shown as a dot-dashed line in Fig. 2) that yields the excitation field components $\mathcal{E}_{2,k}(t)$ ($k=v+2$), is a smoothly varying function of v . In contrast, the time dependence of the resulting total (dump) electric field $E_D(t)$ in Eq. (2) appears very complicated due to its many frequency components.

B. The dynamical parameters

The most important parameters that enter the SAP process are the molecular vibrational period, τ_{vib} (≈ 300 fs for Na_2), the inverse Rabi frequencies $1/\Omega_i$, the pulse length τ_{pulse} , the dephasing time $\tau_{dephase}$, and the radiative decay time τ_{rad} . We find that for the execution of a complete population transfer these dynamical variables must obey the ordering $\tau_{vib} \ll 1/|\Omega_{2,k}| \ll \tau_{pulse} < \tau_{dephase} < \tau_{rad}$. The first inequality follows from our desire to reduce $\Omega_{2,k}$ so as to minimize the Stark shifts of the levels during the laser pulses. The reduction in $\Omega_{2,k}$, in combination with many Rabi oscillations needed in each pulse, requires that for Na_2 , $\tau_{pulse} \geq 20-30$ ps. In order for the superposition state to be generated before its phases are dephased away, $\tau_{pulse} < \tau_{dephase}$. Also, since we want only one initial state to be excited, the (Na_2) molecule should be sufficiently cold so as to populate only a single rovibrational state.

Another deleterious effect is due to anharmonicity of the molecular vibrational system, which causes additional “spreading” of phases in the target superposition state. It is nevertheless possible to adjust the phases of the Rabi frequencies so that the resulting superposition state would replicate the desired target state at a chosen time point t_r . The phase adjustments are determined by including additional phase factors $e^{i\Delta\phi_{2,k}}$, exactly given as $\Delta\phi_{2,k} = \omega_{2,k}t_r$, in the $\mathcal{E}_{2,k}(t)$ field components. The phases $\Delta\phi_{2,k}$ can be estimated by performing a Dunham-type expansion [38] of the oscillator eigenenergies in ($v=k-2$). The first term is the harmonic approximation. The second-order term, reflecting the quadratic corrections, brings about a phase correction of $f_v(\Delta v)^2 t_r$, where for example, for Na_2 , $f_{v=9} \approx -94.7$ μeV . In addition to this effect, in the anharmonic case, the Franck-Condon factors do not strictly follow the dependence shown in Fig. 2.

C. Numerical tests

We have tested the SAP theory by comparing the adiabatic and exact wave-packet dynamics [$\Omega_{2,k}$ vs $\Sigma_{2,k}$ in Eq. (7)] performed on the Na_2 molecule. We consider resonant excitation by two pulses whose Rabi frequencies are Gaussian, $\Omega_{1,2}(t) = \mathcal{O}_{1,2} \exp[-(t-t_0)^2/\tau_{pulse}^2]$ and $\Omega_{2,k}(t) = \mathcal{O}_{2,k} \exp[-t^2/\tau_{pulse}^2]$. Here $\mathcal{O}_{1,2} = |\mathcal{O}_{1,2}| e^{i\phi_{1,2}}$ and $\mathcal{O}_{2,k} = |\mathcal{O}_{2,k}| e^{i\phi_{2,k}}$ are the peak Rabi frequency, $\tau_{pulse} = 30$ ps and $t_0 = 2\tau_{pulse}$ is the delay between the pulses. We set

$$|\mathcal{O}_{1,2}| = |\mathcal{O}_{2,v=9}| = 15/\tau_{pulse} = 0.5 \text{ ps}^{-1},$$

$$|\mathcal{O}_{2,v \neq 9}| = 0.5(9!/v!)^{1/2}(-3)^{v-9}, \quad (20)$$

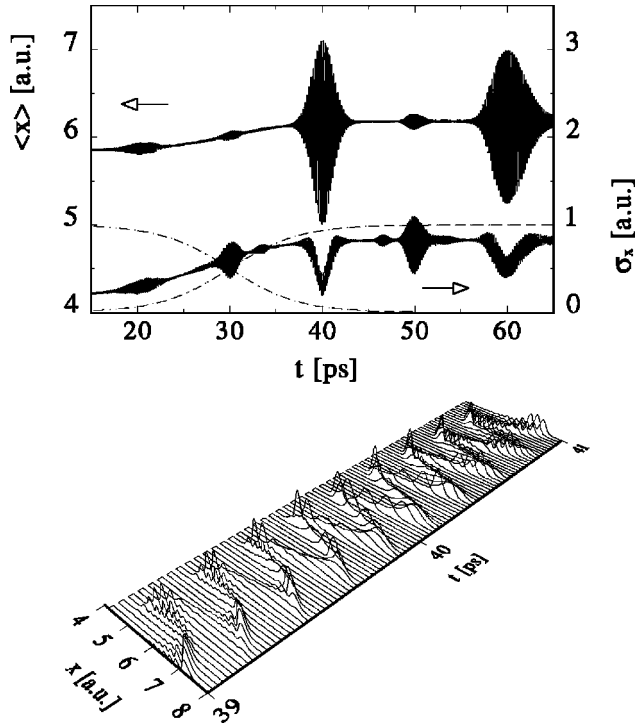


FIG. 3. Upper frame: The time-dependent average position $\langle x(t) \rangle$ (left scale) and the variance $\sigma_x(t)$ (right scale) of a vibrational wave packet created by two pulses, with $|\mathcal{O}_{1,2}|, |\mathcal{O}_{2,v=9}|, |\mathcal{O}_{2,v \neq 9}|$ given in Eq. (20). Phase corrections with $t_r=40$ ps were applied. The two thin dot-dashed lines show the p_1 and $\Sigma_{k=3}^{n+2} p_k$ populations. Lower frame: The wave-packet evolution at around $t=40$ ps.

in accordance with Fig. 2 and Eq. (18). To account for the Na_2 anharmonicities, the initial phases $\phi_{2,k}$ are modified according to $\Delta\phi_{2,k}$. In Na_2 , the laser intensity corresponding to a Rabi frequency of $\mathcal{O}_{1,2}=15/\tau_{pulse}$ is 0.83 MW/cm^2 . This rather low value is due to the large value of $\bar{\mu}$, which, for the $A \leftarrow X$ transition in Na_2 , is $\sim 7 \text{ D}$. Obviously, for other molecules with smaller dipole moments, higher intensities would be required in order to successfully accomplish a complete population transfer.

In Fig. 3 we present (upper curve, left scale) the time-dependent average position $\langle x(t) \rangle$ and (lower curve, right scale) the variance $\sigma_x(t) = \{\langle x^2(t) \rangle - \langle x(t) \rangle^2\}^{1/2}$ of a vibrational wave packet created by exciting the ground Na_2 state by a pulse whose field components are depicted in Fig. 2. In addition, an anharmonic phase correction parameterized by $t_r=40$ ps was applied. For this case, the exact numerical solution, using the full $\Sigma_{2,k}(t)$ of Eq. (7), is practically indistinguishable from the adiabatic solution with $\Omega_{2,k}(t)$. Only when the pulse length τ_{pulse} is too short with respect to τ_{vib} or simply the field intensities are substantially increased, so that $\tau_{vib} \ll 1/|\Omega_{2,k}|$ is no longer correct, significant deviations between the exact numerical solution and the adiabatic approximation show up (see Fig. 4).

The time evolution depicted in Fig. 3 shows an initial rise in $\langle x(t) \rangle$ and in $\sigma_x(t)$ as the $|v>0\rangle \leftarrow |v=0\rangle$ transitions begin to take place. As the system nears the $t_r=40$ ps mark, where the anharmonic dephasings are exactly compensated

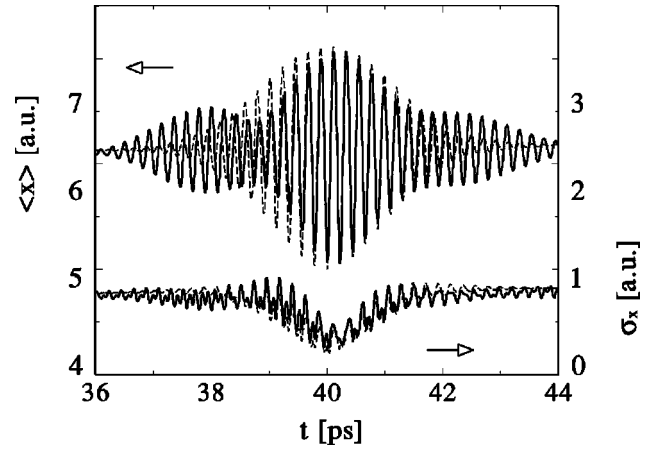


FIG. 4. The average position $\langle x(t) \rangle$ and the variance $\sigma_x(t)$ obtained from the adiabatic solution (broken lines) and from the exact solution (full lines), for strong pulses, $|\mathcal{O}_{1,2}|=|\mathcal{O}_{2,v=9}|=250/\tau_{pulse}$, with $|\mathcal{O}_{2,v \neq 9}|$ being accordingly also 16.6 times their values of Eq. (20). All the other parameters are as in Fig. 3

for, the wave packet becomes highly localized, as evidenced by a sudden drop in the r.m.s. deviation, while undergoing classical-like oscillations, shown more clearly in the lower frame. Following a “fractional revival” [40,41] at 50 ps, at which time the wave packet splits into two (thereby becoming a macroscopic quantum interference or “Schrödinger cat” state [42–45]), an essentially complete revival is seen to occur at 60 ps time.

In Fig. 4 we compare the adiabatic ($\Omega_{2,k}$) and the exact ($\Sigma_{2,k}$) time evolution, around the $t_r=40$ ps time mark, for 16.6 times stronger fields, $|\mathcal{O}_{1,2}|=|\mathcal{O}_{2,9}|=250\tau_{pulse}$ (intensity of 230 MW/cm^2). The strength of the interaction enhances the off-resonance highly oscillatory components of $\Sigma_{2,k}$, so that $\tau_{vib} \ll 1/|\Omega_{2,k}|$ is *not* more valid and the (internal) adiabaticity is broken by Stark shifts of the levels. Although at around the 40 ps time mark the adiabatic solution is in good agreement with the exact one, it gets out of step from it, both in magnitude and phase, after some five vibrational periods. In spite of this, complete population transfer is still possible, since we break only the “internal” adiabaticity, i.e., induce transitions *between* the final levels, and preserve the adiabaticity of the Raman transition $1/|\Omega_{2,k}| \ll \tau_{pulse}$. Therefore, the only difference from the weaker pulse case is that the c_k coefficients are now no longer strictly proportional to the $\Omega_{2,k}$ Rabi frequencies.

D. Sensitivity of SAP to level detuning

In Fig. 5 we investigate the dependence of the detunings of the individual final levels relative to the field components. For simplicity, we consider just *two* final states [32,33], with populations p_3 and p_4 , but the results apply to any pair of levels in a SAP with arbitrary n . We assume that the amplitudes of Rabi frequencies are the same $|\mathcal{O}_{1,2}|=|\mathcal{O}_{2,3}|=|\mathcal{O}_{2,4}|=25/\tau_{pulse}$ and $\tau_{pulse}=30$ ps, with roughly 25 Rabi oscillations in the transition region, and approximate $\Sigma_{2,k}(t)$ by $\Omega_{2,k}(t)$. We slightly detune one of the final states by an amount defined as, $\Delta_{2,4}=\omega_{2,4}-\omega_2+\omega_4$, and plot (thick line) the populations p_3 and p_4 as a function of $\Delta_{2,4}$.

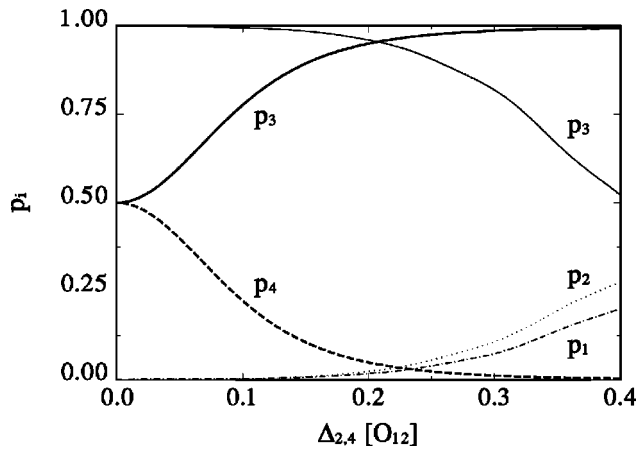


FIG. 5. Thick lines, final populations p_3 and p_4 for equal Rabi frequencies and unequal detuning $\Delta_{2,4} \neq \Delta_{2,3} = 0$. The thin lines show that p_{1-3} populations in the usual STIRAP to a single final state as a function of the $\Delta_{2,3}$ detuning.

We see that for a nonzero detuning, the final probabilities are no longer strictly proportional to the Rabi frequencies. Already for $\Delta_{2,4} = 0.1 \mathcal{O}_{1,2}$, nearly 75% of the populations goes to the resonantly tuned level $|n_1\rangle$, keeping $\approx 25\%$ on the detuned level $|n_2\rangle$. When the Rabi frequencies are doubled to $50/\tau_{pulse}$, the probabilities, though appearing to coincide with those of Fig. 5, are actually less sensitive to the detuning, because the latter is now twice as large. Thus the robustness of SAP with respect to detunings increases with the field intensity.

These results can be compared with the degree of sensitivity of the usual STIRAP scenario (i.e., adiabatic passage to a *single* final state), represented by the thin lines of Fig. 5. We see that the population transfer to a single final state $|3\rangle$ is much less sensitive to the detuning $\Delta_{2,3} = \omega_{2,3} - \omega_2 + \omega_3$. As in SAP, for larger Rabi frequencies the relative sensitivity is further reduced.

In pulse-shaping experiments, proper tuning can be achieved by adjusting the placements of the liquid-crystal elements [22,24] relative to the dispersed pulse so as to introduce only those field components that are in exact resonance with some $\omega_{2,k}$ transition frequency. Recently, STIRAP was also realized with *one* laser beam [46], while the other transition was induced by a tuned vacuum in a high-quality cavity. In SAP, one could generalize this principle and use a cavity with a *structured surface*, which would guide the population in different final states.

IV. CONCLUSION

We have shown that essentially complete population transfer to a sculpted wave packets of any desired makeup can be achieved by a “counterintuitive” pump-dump adiabatic-passage process. The utility of this result is in the simple prescription for pulse shaping it presents. We shape the strong dump pulse in exactly the same manner as dictated by the first-order perturbation theory, namely, its monochromatic field components should be proportional to the complex target expansion coefficients divided by the respective transition dipole matrix elements from the intermediate state to the final states. Therefore, we believe that the SAP scheme can be used in efficient coding of information.

The resulting “shaped-adiabatic-passage” scheme has been computationally tested for the Raman generation of sculpted wave packet on the ground electronic state of the Na_2 molecule. We have shown that the scheme works with pulses of 20–30 ps durations at moderate intensities of a few MW/cm^2 .

ACKNOWLEDGMENTS

We acknowledge support from the Minerva Foundation, the BMBF Strategic Cooperation Project, the German-Israeli Foundation, the EU IHP program HPRN-CT-1999-00129.

-
- [1] M. Shapiro and P. Brumer, *J. Chem. Phys.* **84**, 4103 (1986).
 [2] M. Shapiro and P. Brumer, in *Advances in Atomic, Molecular, and Optical Physics*, edited by B. Bederson and H. Walther (Academic Press, San Diego, 1999), Vol. 42, pp. 287–343.
 [3] D.J. Tannor and S.A. Rice, *J. Chem. Phys.* **83**, 5013, (1985); D.J. Tannor and S.A. Rice, *Acc. Chem. Res.* **70**, 441 (1988).
 [4] A.P. Peirce, M.A. Dahleh, and H. Rabitz, *Phys. Rev. A* **37**, 4950 (1988); W.S. Warren, H. Rabitz and M.A. Dahleh, *Science* **259**, 1581 (1993).
 [5] R. Kosloff, S.A. Rice, P. Gaspard, S. Terisigni, and D.J. Tannor, *Chem. Phys.* **139**, 201 (1989).
 [6] M. Shapiro and P. Brumer, *Chem. Phys. Lett.* **208**, 193 (1993).
 [7] B. Kohler, J.L. Krause, F. Raksi, C. Roseptruck, K.R. Wilson, V.V. Yakovlev, R.M. Whitnell, Y.J. Yan, and S. Mukamel, *J. Phys. Chem.* **97**, 12 602 (1993).
 [8] I. Sh. Averbukh, V.A. Kovarsky and N.F. Perelman, *Phys. Lett. A* **70**, 289 (1979).
 [9] J.A. Yeazell and C.R. Stroud, Jr., *Phys. Rev. A* **35**, 2806 (1986).
 [10] G. Alber, H. Ritsch, and P. Zoller, *Phys. Rev. A* **34**, 1058 (1986); W.A. Henle, H. Ritsch, and P. Zoller, *ibid.* **36**, 683 (1987); G. Alber and P. Zoller, *ibid.* **37**, 377 (1988).
 [11] R. Bluhm and V.A. Kostelecký, *Phys. Rev. A* **48**, R4047 (1993).
 [12] I. Bialynicki-Birula, M. Kaliński, and J.H. Eberly, *Phys. Rev. Lett.* **73**, 1777 (1994); M. Kaliński and J.H. Eberly, *Phys. Rev. A* **53**, 1715 (1996).
 [13] D.W. Schumacher, J.H. Hoogenraad, D. Pinkos, and P.H. Bucksbaum, *Phys. Rev. A* **52**, 4719 (1995).
 [14] J.L. Krause, K.J. Schafer, M. Ben-Nun, and K.R. Wilson, *Phys. Rev. Lett.* **79**, 4978 (1997).
 [15] T.S. Rose, M.J. Rosker, and A.H. Zewail, *J. Chem. Phys.* **88**, 6672 (1988).
 [16] C.C. Hayden and D.W. Chandler, *J. Chem. Phys.* **103**, 10 465 (1995).
 [17] M. Papanikolas, R.M. Williams, P.D. Kleiber, J.L. Hart, C.

- Brink, S.D. Price, and S.R. Leone, *J. Chem. Phys.* **103**, 7269 (1995); R.M. Williams, J.M. Papanikolas, J. Rathje, and S.R. Leone, *Chem. Phys. Lett.* **261**, 405 (1996); R. Uberna, Z. Amitay, C.X.W. Qian, and S.R. Leone, *J. Chem. Phys.* **114**, 10 311 (2001).
- [18] V. Blanchet, M.A. Bouchene, O. Cabrol, and B. Girard, *Chem. Phys. Lett.* **233**, 491 (1995).
- [19] S.B. Fleischer, B. Pevzner, D.J. Dougherty, H.J. Zeiger, G. Dresselhaus, M.S. Dresselhaus, E.P. Ippen, and A.F. Hebard, *Appl. Phys. Lett.* **71**, 2734 (1997).
- [20] C.J. Bardeen, J.W. Che, K.R. Wilson, V.V. Yakovlev, P.J. Cong, B. Kohler, J.L. Krause, and M. Messina, *J. Phys. Chem.* **101**, 3815 (1997).
- [21] T. Baumert, J. Helbing, G. Gerber, L. Wöste, A.H. Zewail, J. Troe, J. Manz, T. Kobayashi, V.S. Letokhov, U. Even, M. Chergui, D.M. Neumark, and S.A. Rice, in *Chemical Reactions and Their Control on the Femtosecond Time Scale XXth Solvay Conference on Chemistry* (Wiley, New York, 1997), Vol. 101, pp. 47–82.
- [22] A.M. Weiner and J.P. Heritage, *Rev. Phys. Appl.* **22**, 1619 (1987); A.M. Weiner, *Rev. Sci. Instrum.* **71**, 1929 (2000).
- [23] M. Haner, and W.S. Warren, *Appl. Phys. Lett.* **52**, 1459 (1988); C.W. Hillegas, J.X. Tull, D. Goswami, D. Strickland, and W.S. Warren, *Opt. Lett.* **19**, 737 (1994).
- [24] A.M. Weiner, D.E. Leaird, G.P. Wiederrecht, K.A. Nelson, *Science* **247**, 1317 (1990).
- [25] R.S. Judson and H. Rabitz, *Phys. Rev. Lett.* **68**, 1500 (1992).
- [26] J. Ortigoso, *Phys. Rev. A* **57**, 4592 (1998).
- [27] T. Assion, T. Baumert, M. Bergt, T. Brixner, B. Kiefer, V. Seyfried, M. Strehle, and G. Gerber, *Science* **282**, 919 (1998).
- [28] D. Grischkowsky and M.M.T. Loy, *Phys. Rev. A* **12**, 1117 (1975); *ibid.* **12**, 2514 (1975).
- [29] A. Kuhn, G.W. Coulston, G.Z. He, S. Schieman, K. Bergmann, and W.S. Warren, *J. Chem. Phys.* **96**, 4215 (1992).
- [30] For recent reviews see, K. Bergmann, H. Theuer, and B.W. Shore, *Rev. Mod. Phys.* **70**, 1003 (1998); N.V. Vitanov, M. Fleischhauer, B.W. Shore, and K. Bergmann, *Adv. At., Mol., Opt. Phys.* **46**, 55 (2001).
- [31] M. Shapiro, *Phys. Rev. A* **54**, 1504 (1996).
- [32] G.W. Coulston and K. Bergmann, *J. Chem. Phys.* **96**, 3467 (1992); R. Unayan, M. Fleischhauer, B.W. Shore and K. Bergmann, *Opt. Commun.* **155**, 144 (1998).
- [33] M.N. Kobrak and S.A. Rice, *Phys. Rev. A* **57**, 2885 (1998).
- [34] P. Král, J. Fiurásek and M. Shapiro, *Phys. Rev. A* **64**, 023414 (2001).
- [35] P. Král and M. Shapiro, *Phys. Rev. Lett.* **87**, 183002 (2001).
- [36] D.G. Abrashkevich, I. Sh. Averbukh, and M. Shapiro, *J. Chem. Phys.* **101**, 9295 (1994).
- [37] P. Král, *J. Mod. Opt.* **37**, 889 (1990); *Phys. Rev. A* **42**, 4177 (1990).
- [38] G. Herzberg, *Molecular Spectra and Molecular Structure: I. Spectra of Diatomic Molecules* 2nd ed. (Van Nostrand, Princeton, 1950).
- [39] W.J. Stevens, M.M. Hessel, P.J. Bertoncini, and A.C. Wahl, *J. Chem. Phys.* **66**, 1477 (1977).
- [40] I. Sh. Averbukh and N.F. Perelman, *Phys. Lett. A* **139**, 449 (1989); *Zh. Éksp. Teor. Fiz.* **96**, 818 (1989) [*Sov. Phys. JETP* **69**, 464 (1990)].
- [41] J.A. Yeazell, M. Mallalieu, and C.R. Stroud, *Phys. Rev. Lett.* **64**, 2007 (1990); J.A. Yeazell and C.R. Stroud, *Phys. Rev. A* **43**, 5153 (1991).
- [42] J.H. Eberly, N.B. Narozhny, and J.J. Sanchez-Mondragon, *Phys. Rev. Lett.* **44**, 1323 (1980).
- [43] G.J. Milburn, *Phys. Rev. A* **33**, 674 (1986); G.J. Milburn and C.A. Holmes, *Phys. Rev. Lett.* **56**, 2237 (1986).
- [44] B. Yurke and D. Stoler, *Phys. Rev. Lett.* **57**, 13 (1986).
- [45] A. Mecozzi and P. Tombesi, *Phys. Rev. Lett.*, **58**, 1055 (1987).
- [46] M. Hennrich, T. Legero, A. Kuhn, and G. Rempe, *Phys. Rev. Lett.* **85**, 4872 (2000).